Preparation and Characterization of Maleic Anhydride Grafted Poly (Hydroxybutirate-CO-Hydroxyvalerate) – PHBV-*g*-MA

Thaís Larissa do Amaral Montanheiro[a]*, Fábio Roberto Passador[a], Maurício Pinheiro de Oliveira[a],

Nelson Durán[b,c], Ana Paula Lemes[a]

[a]*Instituto de Ciência e Tecnologia , Universidade Federal de São Paulo - UNIFESP,*
Rua Talim, 330, CEP: 12231-280, São José dos Campos, SP, Brazil
[b]*Instituto de Química, Universidade Estadual de Campinas - UNICAMP, CP 6154,*
Rua Carlos Gomes, 241, CEP: 13083-970, Campinas, SP, Brazil
[c]*Laboratory on Nanostructures Synthesis and Biological Interactions - NanoBioss, Universidade*
Estadual de Campinas - UNICAMP, Rua Carlos Gomes, 241,
CEP: 13083-970, Campinas, SP, Brazil

A compatibilizer agent was successfully produced by grafting maleic anhydride (MA) to poly(hydroxybutyrate-*co*-hydroxyvalerate) (PHBV) chains on a reactive processing by mechanical mixing, using a mixture of PHBV, MA and dicumyl peroxide (DCP) as initiator. The resulting PHBV grafted MA (PHBV-*g*-MA) was characterized by Fourier transform infrared (FTIR) spectroscopy, thermogravimetric analysis (TGA), differential scanning calorimetry (DSC) and gel permeation chromatography (GPC), and its properties were compared to neat PHBV. FTIR showed an absorption band at 699 cm^{-1} for PHBV-*g*-MA, related to CH group of grafted anhydride ring. The initial thermal degradation temperature of the compatibilizer agent was reduced when compared to neat PHBV. DSC analysis showed that after grafting MA onto PHBV the crystallization temperature was about 20ºC higher than neat PHBV, and the degree of crystallinity was increased. GPC analysis showed that MA when grafted onto PHBV led to a reduction of molecular weight and polydispersity.

Keywords: *Poly(hydroxybutyrate-co-hydroxyvalerate); Maleic anhydride; Graf copolymer; Compatibilizer, biopolymer*

1. INTRODUCTION

The addition of fillers or nanofillers for reinforcement of polymeric matrixes needs always the analysis of interfacial region between filler and polymer matrix, since the compatibility between these components determines the final properties of composites and nanocomposites [1]. It is through the interfacial region that occur the strain transfer from the matrix to the reinforcement agent. When there is no compatibility, the interfacial region is the weaker region of the composite, and is where the failure occurs, due to inefficient strain transfer [2]. For this reason, many works have as object of study the improvement of compatibility between filler and matrix.

Compatibilizer agents are materials that promote compatibility to incompatible materials, and it results in a material with a reduced interfacial stress [3]. Compatibilization strategies have to be considered to optimize the effects of the reinforcement phase [4].

Several methods have been proposed to increase the interfacial adhesion between the reinforcement agent and the polymer matrix, including fiber modifications [5] and grafting MA to the matrix as compatibilizer [5,6]. Maleic anhydride is highly reactive with a great variety of polymer chains and

biological macromolecules, as protein, lipid and glucose [7]. The MA groups grafted to the polymer may react with the reinforcement agent functional groups, resulting in grafted copolymers. The MA grafted to thermoplastic polymer can increase the polarity, which leads to better adhesion with biofillers [8] that have polar groups on their surfaces.

Some works in the literature have proposed the use of MA grafted to thermoplastics as polyethylene and polypropylene [8–13] to improve the interfacial adhesion between the matrix and some reinforcement agents, as oak wood flour [5], bamboo pulp fiber [14], kenaf fiber [4], clay [6,13,15], bio-flour-filled [8] and others.

It was observed that the presence of the compatibilizer agent induces a stronger interfacial adhesion and improvement of the mechanical properties, compared to uncompatibilized composites [4,15], besides improving the particle dispersion into polymer matrix [13], and the thermal stability of composite [8].

For the bio-flour-filled polypropylene composites with MA functionalized polypropylene as compatibilizing agent, the authors observed improved mechanical and thermal stability and interfacial adhesion [8]. The polyethylene/clay nanocomposites produced with polyethylene grafted to MA (PE-*g*-MA) as compatibilizer were compared to other produced with oxidized polyethylene (Ox-PE) as compatibilizer.

*e-mail: thais.montanheiro@unifesp.br

The results showed better clay dispersion and more exfoliated structure for the nanocomposite produced with PE-*g*-MA as compatibilizer [13]. Passador et al., [16] studied the influence of two different compatibilizers agents and their combination (MA grafted high density polyethylene, HDPE-*g*-MA; MA grafted linear low density polyethylene, LLDPE-*g*-MA; and 50/50 wt% mixture of these compatibilizers) on the rheological, thermo-mechanical and morphological properties of HDPE/LLDPE/organoclay blend-based nanocomposites. In this study, compatibilized nanocomposites exhibited an intercalated morphology with a small number of individual platelets dispersed in the HDPE/LLDPE matrix and the mechanical performance of the system was not governed only by the clay exfoliation and clay content but also by the presence of a significant amount of the compatibilizer agent.

Polyhydroxyalkanoates (PHA) are a family of biodegradable polyesters which are naturally synthesized by microorganisms from several carbon substrates, and exist inside the cell as granules, as carbon or energy storage. PHBV is a straight-chain semicrystalline copolymer from PHA family with smaller amount of hydroxyvalerate (HV) units and higher proportion of hydroxubutyrate (HB) units. PHA can be depolymerized by hydrolysis reactions, at which the molecules of water cause the scission of ester bonds, producing carboxylic acid and alcohol groups. The biodegradation of PHA can occur inside the cell, by microorganisms that produce PHA, or outside the cell by microorganisms that do not produce PHA, but can also use it as carbon and energy sources. However, in both cases the hydrolysis is catalyzed by specific enzymes, intracellular, or extracellular PHA depolymerases [17].

PHBV have attracted much attention as environmentally degradable polymer, which are useful for a wide range of applications. No special attention was given to the compatibilizer agent, and the changes that the MA may cause to the graft polymer. Furthermore few studies have reported the changes that grafting MA caused to biodegradable polymers, as poly(hydroxybutyrate), PHB and PHBV, as did the work of Chen et al., [18] where the authors compared the non isothermal crystallization and melting behavior of PHB and maleated PHB, PHB-*g*-MA, by DSC using different cooling rates. The authors showed that the crystallization and melting behaviors of PHB and PHB-*g*-MA are affected by the cooling rates and degree of grafting.

In another study, Chen et al. employed MA as the grafting monomer to be grafted onto PHB chains. Authors supposed that introducing MA onto PHB chains could disturb the regularity of PHB chains, then control the morphological structures and improve its properties [19].

The grafting reaction of PHBV occurs in two stages showed in Figure 1. In the first stage the alkyl radical is produced, using dicumyl peroxide (DCP) as initiator, and in the second stage the compatibilizer agent is produced,
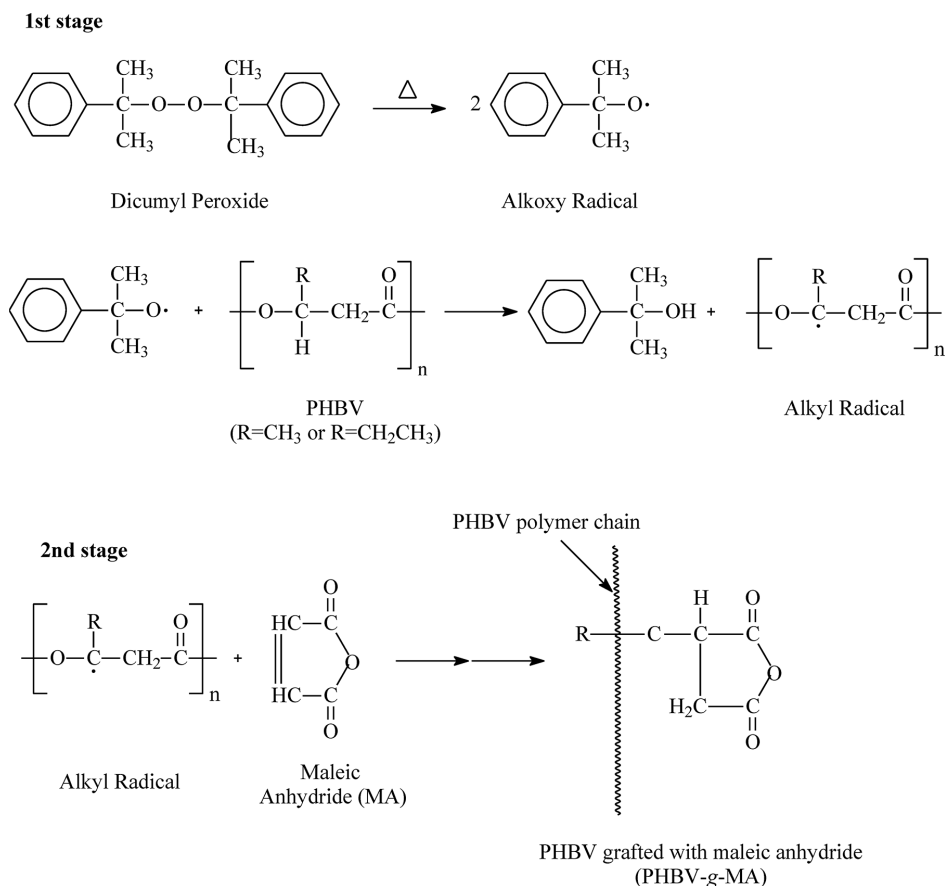
Figure 1. Reaction scheme of grafting reactions between MA and PHBV in presence of DCP.

by grafting MA to PHBV chains. The purpose of this work was to produce a MA grafted poly(hydroxybutyrate-*co*-hydroxyvalerate), PHBV-*g*-MA, and evaluate its structural and thermal characteristics.

2. EXPERIMENTAL

2.1. Materials

Poly(3-hydroxybutyrate-*co*-3-hydroxyvalerate) was provided by PHB Industrial, Brazil, with 15 mol % of hydroxyvalerate units and average molecular weight (*Mw*) of 159.000 g mol⁻¹, average number molecular weight (*Mn*) of 61.100 g mol⁻¹ and PDI of 2.60. The material was used as received. Maleic anhydride (MA) from Aldrich with 99% of purity and dicumyl peroxide (DCP) from Aldrich with minimum 98% of purity were used as received.

2.2. Grafting of MA to PHBV

The grafting reaction of MA to PHBV chains was made by reactive processing in a torque rheometer (Haake 600). In this procedure, a mixture of PHBV and MA at the ratio of 90:10 (w/w) and 6% (w/w_PHBV) of DCP was mixed in the molten state operated at 175ºC, 50 rpm during 5 min using counter-rotation and interpenetrated rotors [20].

2.3. Characterization

2.3.1. FTIR spectroscopy

FTIR spectroscopy analysis was performed using a Shimadzu IR Affinity-1 Spectrometer, with 2 cm⁻¹ resolution to confirm the grafting reaction between PHBV and maleic anhydride. Samples were prepared into potassium bromide (KBr) disks.

2.3.2. Thermogravimetric analysis (TGA)

The thermal stability of neat PHBV and PHBV-*g*-MA was evaluated by thermogravimetric analysis, using a simultaneous TGA/DSC Analyser SDT Q600 from TA Instruments. Samples were heated from room temperature to 1000°C with a heating rate of 10°C min⁻¹, under nitrogen atmosphere with a flow rate of 100 mLmin⁻¹.

2.3.3. Differential scanning calorimetry (DSC)

The crystallization and melting behaviors of neat PHBV and PHBV-*g*-MA were characterized by DSC using a TA Instruments Q10 equipment. Samples were sealed in an aluminum DSC pan and heated from room temperature to 200 °C at 10 °C min⁻¹.They were kept at 200°C for 2 min to eliminate the heat history, subsequently cooled to -20°C at 10°C min⁻¹, and kept at this temperature during 1 min. After this, they were heated to 200°C at 10°C min⁻¹. The analyses were performed under nitrogen atmosphere with a flow rate of 50 mL min⁻¹. The degree of crystallinity, X_c (%) was calculated according to Equation 1, where ΔH_{m1} is the total melting enthalpy on second heating, W_{PHBV} is the weight fraction of PHBV in the sample and ΔH_m^0 is theoretical melting heat value of 100% crystalline PHBV, which was taken as 109 J g⁻¹ [21].

$$X_c\,(\%) = \frac{\Delta H_{m1}}{W_{PHBV} \cdot \Delta H_m^0} * 100 \qquad (1)$$

2.3.4. Gel Permeation Chromatography (GPC)

The weight and number-average molecular weights (*Mw and Mn*) and the polydispersity index (PDI) for PHBV and PHBV-*g*-MA polymers were measured by GPC (Waters) equipped with a Waters 1515 HPLC pump, a Waters 2414 refractive index detector, a Waters Plus 717 autosampler and a Viscotek 302 dual detector. Polystyrene standards were used to calibrate the dual detector, and set of PLgel, (Phenomenex) column oven with porosities of 10³, 10⁴ and 10⁶ Å. Each polymer sample was dissolved in chloroform in a concentration of 0.8 g L⁻¹, prepared at 35ºC overnight to allow full dissolution in oil bath and then filtered through a 0.45 μm polytetrafluoroethylene (PTFE) syringe filter (Millex LCR). The eluent was chloroform at a flow rate of 1.0 mL min⁻¹ and temperature of 30°C. The molecular weight and PDI (*Mw/Mn*) values were derived from a calibration curve based on narrow polystyrene standards.

3. RESULTS AND DISCUSSION

3.1. FTIR spectroscopy

Figures 2 and 3 show a comparison between the infrared spectrum of neat PHBV and PHBV grafted with 10% (w/w) of MA (PHBV-*g*-MA). All the characteristic peaks of neat PHBV can also be observed on PHBV-*g*-MA spectrum on Figure 2, as the peaks at 2975 and 2937 cm⁻¹ that are attributed to symmetric and asymmetric stretching of CH₃ group, and at 1725 cm⁻¹ which refers to carbonyl stretching (C=O) of PHBV [22]. The peaks present between 1500 and 900 cm⁻¹ related to CH₃ and CH vibrations and C-O-C and C-C stretching are also observed [23].

Figure 3 shows the region between 900 and 500 cm⁻¹, where is possible to suggest that MA is grafted to PHBV chains, due to the appearance of a new absorption band at 699 cm⁻¹, which is attributed to the bending of the CH group of grafted anhydride ring [4].
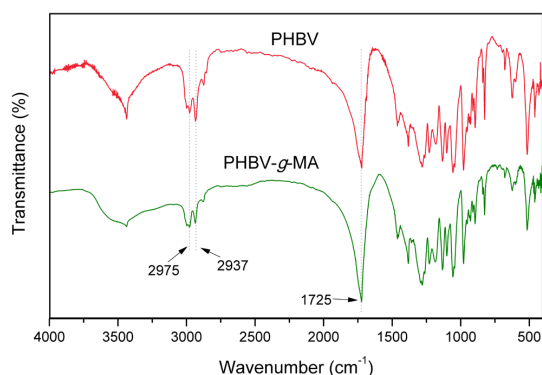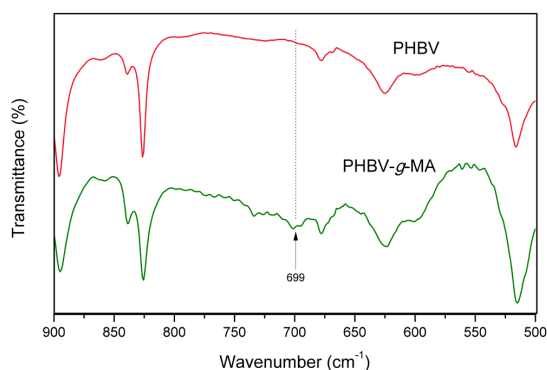

**Figure 2.** FTIR spectroscopy of neat PHBV and PHBV-*g*-MA.

3.2. Thermogravimetric Analysis

Thermal degradation behaviors for neat PHBV and PHBV-*g*-MA are shown on Figure 4, where can be observed that both neat PHBV and PHBV-*g*-MA have a very similar thermal decomposition pattern, with little difference only in the beginning of weight loss. In the final stages of weight loss it is possible to observe some differences between the curves, but the thermal degradation temperatures of 1, 10, 65 and 95% (T1%, T10%, T65% and T95%) of weight loss and temperature of maximum weight loss rate (T_{max}) from both samples are close, as shown on Table 1.

The grafting reaction of MA reduces the initial thermal degradation since the values of T1% and T10% of PHBV-*g*-MA are lower than values obtained to PHBV. This is a common behavior due to the presence of MA, which shows low thermal stability like observed for many systems [24]. The values of T65%, T95% and T_{max} are close for both samples, proving that grafting MA to PHBV only influences the outset of the copolymer thermal degradation.
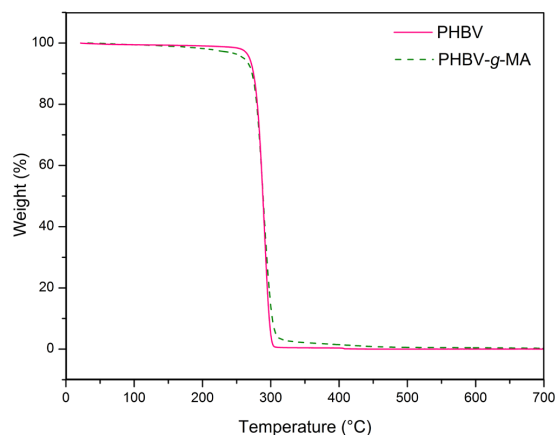
The thermal degradation of PHBV is usually a statistical process based on a random scission mechanism of ester groups [25], with elimination of a β hydrogen [4]. Some kinetically favored scissions occur next to the end of macromolecules chains [25], due to the major conformational freedom and free volume.

From Figure 4 it is possible to observe that the thermal degradation of neat PHBV and PHBV-*g*-MA occur in a single process and from the first derivative curves showed in Figure 5 it is observed that the thermal degradation occur with a temperature of maximum weight loss rate. The temperature of maximum weight loss rate from neat PHBV and PHBV-*g*-MA is the same, indicating that grafting MA to PHBV does not change the maximum weight loss degradation behavior of the PHBV matrix. Thus, thermogravimetric curves indicate that the compatibilizer agent will not be degraded during its processing.

3.3. Differential scanning calorimetry

The grafting reaction of maleic anhydride to PHBV was also evaluated by differential scanning calorimetry, to compare the melting and crystallization behaviors from both samples. The first and second heating curves are shown on Figures 6 (a) and (b), respectively. The values of melting temperature (T_m), melting enthalpy (ΔH_m), crystallization temperature (T_c) and crystallization enthalpy (ΔH_c), degree of crystallinity (X_c) and glass transition temperature (T_g) from second heating scan are shown on Table 2.

In Figure 6 (a), it is observed that PHBV shows bimodal endothermic melting peaks at approximately 156 and 173 ºC. The presence of these peaks is justified by the melting of crystals with different lamellar thickness and/or different crystal structures [26]. For this reason, on second heating scan,

Figure 3. FTIR spectroscopy of neat PHBV and PHBV-g-MA in the region between 900 and 500 cm-1.

Table 1 – Temperatures of 1, 10, 65 and 95% of weight loss and temperature of maximum weight loss rate (T_{max}).

Sample	T1% (°C)	T10% (°C)	T65% (°C)	T95% (°C)	T_{max} (°C)
PHBV	230	277	293	302	291
PHBV-*g*-MA	148	273	293	307	290

Figure 4. Thermal degradation of neat PHBV and PHBV-*g*-MA.
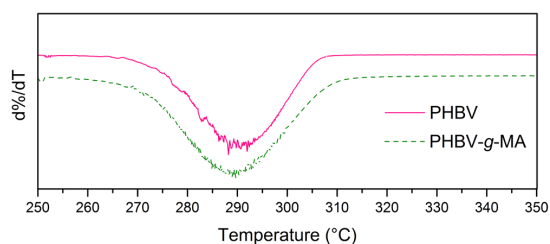
Figure 5. First derivative thermogravimetric curve from neat PHBV and PHBV-*g*-MA.

Table 2. Crystallization temperature (T_c), crystallization enthalpy (ΔH_c), melting temperature (T_m), melting enthalpy (ΔH_m) and glass transition temperature (T_g) on second heating scan for neat PHBV and PHBV-*g*-MA.

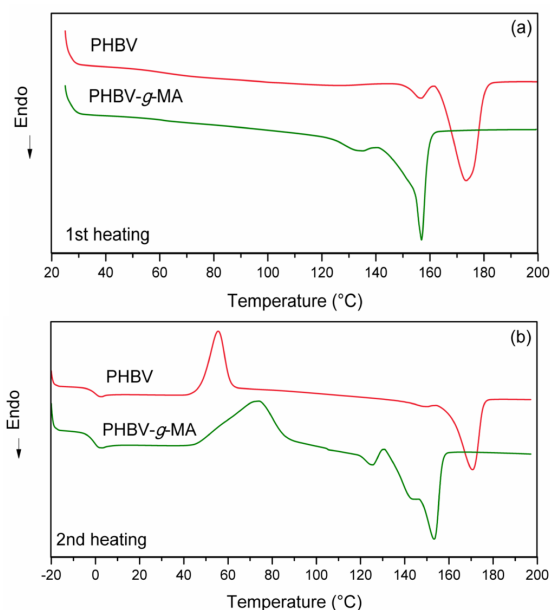| Sample	T_g (°C)	T_c (°C)	ΔH_c (J/g)	T_{m1} (°C)	T_{m2} (°C)	T_{m3} (°C)	ΔH_m (J/g)	Xc (%)
PHBV	0.2	55	39	148	171	-	51	47
PHBV-*g*-MA	-0.3	74	40	126	153	143	50	54

Figure 6. DSC curves for neat PHBV and PHBV-*g*-MA: (a) first heating and (b) second heating

Figure 6 (b), the first endothermic melting peak (156 ºC) is drastically reduced, due to the controlled cooling and heating rates, which allowed the formation of crystals with higher homogeneity.

The crystallization behavior for both samples is observed during the second heating scan, as indicated by the exothermic peaks from the curves. Crystallization during the heating scan occurs due to the gain of mobility of the polymer chains, which allows that the polymer chains organize and form the crystals. It may be observed that grafting MA to PHBV does not hinder the crystallization process, but increases almost 20ºC the crystallization temperature. It also may be observed that the crystallization peak for neat PHBV is narrower than for PHBV-*g*-MA, indicating the formation of crystals with more homogeneous size distribution. For PHBV-*g*-MA the crystallization peak is larger, due to the formation of crystals with lower perfection and largest size distribution.

As mentioned previously, the second heating scan shows that the melting peak at lower temperature observed for neat PHBV during the first heating is reduced, indicating that it is related to the cooling rates that the sample is submitted. However, for PHBV-*g*-MA, it is observed the presence of three endothermic melting peaks. In this case, the temperatures are about 20ºC lower compared to neat PHBV, as can be verified on Table 2. Furthermore, it is observed the presence of a

new peak at 143ºC (T_{m3}). This new peak indicates that the crystalline fraction of PHBV-*g*-MA is greatly heterogeneous, compared to neat PHBV.

The grafting reaction of MA causes great changes on PHBV structure, increasing the values of crystallinity degree (X_c), but with large crystal size distribution.

The second heating scan also shows the drop on the baseline for neat PHBV and for PHBV-*g*-MA, which indicates the glass transition temperature (T_g), arising from changes in heat capacity of the material, due to the mobility of the chains on the amorphous phase. This drop happens sharply in a small temperature range. For neat PHBV, T_g is 0.2°C and for PHBV-*g*-MA the value is -0.3°C, indicating no significant difference between T_g values.

3.4. Gel permeation chromatography

The weight average molecular weight (*Mw*), number average molecular weight (*Mn*), and polydispersity index (PDI) of PHBV and PHBV-*g*-MA polymers are presented in Table 3. PHBV-*g*-MA sample had a much lower *Mw* and *Mn* than neat PHBV processed without the addition of MA. PHBV-*g*-MA polymer had larger PDI when compared to neat PHBV. This decrease of *Mw* and *Mn* could be attributed to the chain scission of PHBV chains induced by hydrolysis reactions in the PHBV-*g*-MA polymer. Higher amount of MA leads to a higher radical molecule concentration that could induce macromolecular scission of PHBV, significantly reducing the molecular weight and increasing the PDI [27].

On the other hand, the process conditions employed could be also responsible for a decrease of the PHBV-*g*-MA molecular weight and larger PDI. This behavior suggests a higher rate of degradation of PHBV as function of the MA amount and process conditions employed. Avella et al., [4] reported similar results. The authors observed that the MA amount and process conditions had a negative effect on the molecular weight of PHBV-*g*-MA. According to the authors, the molecular weight of PHBV grafted with MA decreased by chain scission of PHBV due to hydrolysis and thermal degradation.

For polypropylene grafted with maleic anhydride (PP-*g*-MA), produced by melt processing or reactive extrusion, the reduction of *Mw* is also observed, due to the cleveage of C-C backbone bonds [28]. Shi et al., [12] reported reduction in *Mw* of about 70% for PP-*g*-MA, compared to neat PP. Polypropylene is a thermally stable polymer and suffers reduction of molecular weight when processed at high temperatures. For PHBV this behavior is more pronounced, since it is not thermally stable.

Although there is a reduction of PHBV-*g*-MA molecular weight, the polymer remained thermally stable, as shown by thermogravimetric analysis. The increase on the values of

Sample	M_w (g mol $^{-1}$)	M_n (g mol $^{-1}$)	PDI (M_w/M_n)
PVBV	158.940	61.140	2.60
PHBV-*g*-MA	16.260	5.640	2.90

crystallinity for PHBV-*g*-MA may be assigned to PHBV chain scission, which led to smaller polymer chains with easier packing, resulting higher values of crystallinity. Simultaneously, the increase of PDI values affect the crystal size distribution, observed on DSC for PHBV-*g*-MA. The appearance of a new peak at 143°C on the second heating scan for the MA grafted sample confirms that the crystalline fraction for this sample is greatly heterogeneous, compared to neat PHBV.

4. CONCLUSIONS

This paper has reported a method to produce a compatibilizer agent, by grafting MA to PHBV chains. The proposed method was efficient for the expected results, and it was

confirmed on the infrared spectroscopy, which showed a new absorption band at 699 cm^{-1} for PHBV-*g*-MA, related to the bending of the CH group of grafted anhydride ring. Thermal analyses showed that the grafting reaction of MA reduces the initial weight loss temperature in about 80ºC for 1% of weight loss, but does not change the main degradation behavior of the PHBV matrix. The crystallization process was retarded in about 20ºC with the grafting of MA, and the crystalline fraction was increased. The presence of MA grafted to PHBV led to a reduction of molecular weight and a larger PDI. This effect was attributed to the formation of a higher number of PHBV chains scission during processing. The grafting of MA using the proposed methodology may be an alternative to produce polymers with lower molecular weight, without impairing its thermal stability.

REFERENCES

1. Hussain F. Polymer-matrix nanocomposites, processing, manufacturing, and application: an overview. *Journal of Composite Materials*. 2006;40(17):1511-1575.

2. Oliveira TÁ, Teixeira A, Mulinari DR, Goulart SA. Avaliação do uso de agente compatibilizante no comportamento mecânico dos compósitos PEBD reforçados com fibras de coco verde. *Cadernos UniFOA*. 2010;14:11-17.

3. Carraher CE. *Polymer Chemistry*. 8th ed. Boca Raton: CRC Press; 2011.

4. Avella M, Bogoeva-Gaceva G, Buz A, Errico ME, Gentile G, Grozdanov A. Poly (3-hydroxybutyrate-co-3-hydroxyvalerate)-based biocomposites reinforced with kenaf fibers. *Journal of Applied Polymer Science*. 2007;104(5):3192-3200.

5. Srubar WV, Pilla S, Wright ZC, Cecily AR, Joseph PG, Curtis WF, Sarah LB. Mechanisms and impact of fiber–matrix compatibilization techniques on the material characterization of PHBV/oak wood flour engineered biobased composites. *Composites Science and Technology*. 2012;72(6):708-715. doi:10.1016/j.compscitech.2012.01.021

6. Lee LJ, Zeng C, Cao X, Han X, Shen J, Xu G. Polymer nanocomposite foams. *Composites Science and Tecnology*. 2005;65(15-16):2344-2363.doi:10.1016/j.compscitech.2005.06.016

7. Lu Y-Y, Li H, Liu H-Z. Maleic anhydride functionalization of multi-walled carbon nanotubes by the electron beam irradiation in the liquid media. *Physica E: Low-dimensional Systems Nanostructures*. 2010;43(1):510-514. doi:10.1016/j.physe.2010.09.004

8. Kim H-S, Lee B-H, Choi S-W, Kim S, Kim H-J. The effect of types of maleic anhydride-grafted polypropylene (MAPP) on the interfacial adhesion properties of bio-flour-filled polypropylene composites. *Composites Part A*. 2007;38(6):1473-1482.

9. Yang L, Zhang F, Endo T, Hirotsu T. Microstructure of maleic anhydride grafted polyethylene by high-resolution solution-state NMR and FTIR spectroscopy. *Macromolecules*. 2003;36(13):4709-4718. DOI: 10.1021/ma020527r

10. Seo Y, Kim J, Kim KU, Young CK. Study of the crystallization behaviors of polypropylene and maleic anhydride grafted

polypropylene. *Polymer*. 2000; 41(7):2639-2646.doi:10.1016/S0032-3861(99)00425-5

11. Sclavons M, Franquinet P, Carlier V, Verfaillie G, Fallais I, Legras L, et al. Quantification of the maleic anhydride grafted onto polypropylene by chemical and viscosimetric titrations, and FTIR spectroscopy. *Polymer*. 2000;41(6):1989-1999.

12. Shi D, Yang J, Yao Z, Wang Y, Huang H, Jing W, et al. Functionalization of isotactic polypropylene with maleic anhydride by reactive extrusion: mechanism of melt grafting. *Polymer*. 2001;42(13):5549-5557.

13. Durmus A, Kasgoz A, Macosko CW. Linear low density polyethylene (LLDPE)/clay nanocomposites. Part I: Structural characterization and quantifying clay dispersion by melt rheology. *Polymer*. 2007;48(15):4492-4502.doi:10.1016/j.polymer.2007.05.074

14. Jiang L, Huang J, Qian J, Chen F, Zhang J, Wolcott MP, et al. Study of Poly(3-hydroxybutyrate-co-3-hydroxyvalerate) (PHBV)/bamboo pulp fiber composites: effects of nucleation agent and compatibilizer. *Journal of Polymers and the Environment*. 2008;16(2):83-93.

15. Modesti M, Lorenzetti A, Bon D, Besco S. Effect of processing conditions on morphology and mechanical properties of compatibilized polypropylene nanocomposites. *Polymer*. 2005;46(23):10237-10245.doi:10.1016/j.polymer.2005.08.035

16. Passador FR, Ruvolo-Filho AC, Pessan LA. Effects of different compatibilizers on the rheological, thermomechanical, and morphological properties of HDPE/LLDPE blend-based nanocomposites. *Journal of Applied Polymer Science*. 2013;130(3):1726-1735.DOI: 10.1002/app.39265

17. Lemes AP, Montanheiro TL, Passador FR, Durán N. Nanocomposites of polyhydroxyalkanoates reinforced with carbon nanotubes: chemical and biological properties. In: Thakur VK, Thakur MK, editors. *Eco-friendly Polymer Nanocomposites: processing and properties*. Springer; 2015. p. 79-108. (Advanced Structure Materials, 75).

18. Chen C, Fei B, Peng S, Zhuang Y, Dong L, Feng Z. Nonisothermal crystallization and melting behavior of poly(3-hydroxybutyrate) and maleated poly(3-hydroxybutyrate). *European Polymer Journal*. 2002;38(8):1663-1670.doi:10.1016/S0014-3057(02)00046-0

19. Chen C, Peng S, Fei B, Zhuang Y, Dong L, Feng Z, et al. Synthesis and characterization of maleated poly(3-hydroxybutyrate). *Journal of Applied Polymer Science.* 2003;88(3):659-668. DOI: 10.1002/app.11771

20. Lemes AP. *Desenvolvimento de novos compósitos biodegradáveis baseados em poli(3-hidroxibutirato- co- hidroxivalerato) e lignosulfonatos*. [Dissertation]. Campinas: Brazil: Universidade Estadual de Campinas; 2005.

21. Vidhate S, Innocentini-mei L, Souza NA. Mechanical and Electrical multifunctional poly (3-hydroxybutyrate- co -3-hydroxyvalerate) — multiwall carbon nanotube nanocomposites. *Polymer Engineering & Science.* 2012;52(6):1367-1374. DOI: 10.1002/pen.23084

22. Ke Y, Wu G, Wang Y. PHBV/PAM scaffolds with local oriented structure through UV polymerization for tissue engineering. *BioMed Research International.* 2014; 2014:1-9.

23. Yu H-Y, Yao J-M, Qin Z-Y, Liu L, Yang X-G. Comparison of covalent and noncovalent interactions of carbon nanotubes on the crystallization behavior and thermal properties of poly(3-hydroxybutyrate- co -3-hydroxyvalerate). *Journal of Applied Polymer Science.* 2013;130(6):4299-4307.DOI: 10.1002/app.39529

24. Bhuyan K, Dass NN. Thermal studies of copolymers of styrene and maleic anhydride. *Journal of Thermal Analysis.* 1989;35:2529-2533.

25. Lai M, Li J, Yang J, Liu J, Tong X, Cheng H. The morphology and thermal properties of multi-walled carbon nanotube and poly(hydroxybutyrate-co-hydroxyvalerate) composite. *Polymer International*. 2004;53(10):1479-1484.DOI: 10.1002/pi.1566

26. Gunaratne LM, Shanks RA, Amarasinghe G. Thermal history effects on crystallisation and melting of poly(3-hydroxybutyrate). *Thermochimica Acta.* 2004;423(1-2):127-135.doi:10.1016/j.tca.2004.05.003

27. Rzayev ZM. Graft copolymers of maleic anhydride and its isostructural analogues: high performance engineering materials. *International Review of Chemical Engineering.* 2011;3(2):153-215. http://arxiv.org/ftp/arxiv/papers/1105/1105.1260.pdf

28. Diop MF, Torkelson JM. Maleic anhydride functionalization of polypropylene with suppressed molecular weight reduction via solid-state shear pulverization. *Polymer.* 2013;54(16):4143-4154.doi:10.1016/j.polymer.2013.06.003